# Modeling of thickness dependent infrared radiance contrast of native and crude oil covered water surfaces

**Wei-Chuan Shih and A. Ballard Andrews**

*Schlumberger-Doll Research*
*1 Hampshire Street, MD353*
*Cambridge MA 02139*
*wshih@alum.mit.edu*

**Abstract:** We present a model for infrared radiance contrast of native and crude oil covered water surfaces. This model is based on the so called "direct" approach by treating individual volumetric elements as incoherent radiators. The total emitted radiation is calculated by the sum of individual contributions from the oil film and the underlying water, respectively. Therefore, different temperatures can be assigned to the oil film and water assuming quasi-static temperature distribution, enabling modeling of differential heating of the oil film during daytime. This model can be applied to remote sensing, particularly, to explain the historically observed thickness-dependent contrast in native and crude oil covered sea surfaces.



**OCIS codes:** (260.3060) Infrared; (260.3160) Interference; (280.6780) Temperature.

## References and links

1. M. F. Fingas et al., in *Proceedings of the fifth thematic conference on remote sensing for marine and coastal environments*, Environmental Research Institute of Michigan, Ann Arbor, Michigan, pp. II 411-418, 1998.
2. R. H. Goodman, *The remote sensing of oil slicks*, Lodge AE, ed., (John Wiley and Sons, Chichester, UK, 1989), pp. 39-65.
3. N. Hurfurd, *The remote sensing of oil slicks*, Lodge AE, ed., (John Wiley and Sons, Chichester, UK, 1989), pp. 7-16.
4. U. Hua, "Remote sensing of oil spills in thermal infrared - Contour line effect," in *Proceedings of IEEE International Geoscience and Remote Sensing Symposium* (IEEE 1991) **3**, pp. 1315-1317.
5. R. Horvath et al., "Optical remote sensing of oil slicks: signature analysis and systems evaluation," (The University of Michigan 1971).
6. Z. Otremba, "The impact on the reflectance in VIS of a type of crude oil film floating on the water surface," Opt. Express **7**, 129-134 (2000).
7. R. Siegel and J. R. Howell, *Thermal radiation heat transfer*, 4th ed., (Taylor & Francis 2001).
8. P. Pigeat et al., "Calculation of thermal emissivity for thin films by a direct method," Phys. Rev. B **57**, 9293-9300 (1998).
9. A. Hadni, *Essentials of modern physics applied to the study of the IR* (Paragon, Oxford 1967).
10. M. O. McMahon, "Thermal radiation from partially transparent reflecting bodies," J. Opt. Soc. Am. **40**, 376-380 (1950).
11. V. P. Tolstoy, *Handbook of infrared spectroscopy of ultrathin films* (Wiley 2003).
12. American Petroleum Institute, "American Petroleum Institute research project 44 selected properties of hydrocarbons and related compounds," (Carnegie Institute of Technology 1966).
13. G. M. Hale and M. R. Querry, "Optical constants of water in the 200-nm to 200-µm wavelength region," Appl. Opt. **12**, 555-563 (1973).
14. J. H. W. G. den Boer, G. M. W. Kroesen, and F. J. de Hoog, "Measurement of the complex refractive index of liquid in the infrared using spectroscopic attenuated total reflection ellipsometry: correction for depolarization by scattering," Appl. Opt. **34**, 5708-5714 (1995).

#96040 - $15.00 USD Received 12 May 2008; revised 17 Jun 2008; accepted 27 Jun 2008; published 30 Jun 2008

## 1. Introduction

Remote sensing of crude oil spills on sea surfaces has been of great interest in environmental protection and disaster management. An effective sensor needs to detect contrast between native and thin oil film covered sea surfaces. Optical techniques have been widely employed in environmental monitoring because they can rapidly scan a wide region. Among various optical remote sensing techniques, thermal imaging using long wavelength infrared (LWIR) (8-14 μm) light has been successfully commercialized in recent years partially because of the cost of detector technology has decreased. In addition, since the solar spectrum peaks in the visible (~500 nm), LWIR measurements are much less sensitive to solar interference [1]. An LWIR remote sensing system can be as simple as a thermal camera based on either microbolometer technology or pyroelectric effect. With rapid advancements in focal plane array detector technology, such uncooled devices with ~100 mK thermal sensitivity and standard video stream output are commercially available. In addition, since artificial illumination is not required, the instrument complexity and power budget can be significantly reduced.

In several studies of crude oil spillage, the researchers observed that the apparent day time contrast of native and crude oil covered sea surfaces depends on the thickness of the oil film [1-4]. Because the refractive index of oil is usually larger than water, the bulk emissivity of water is higher than oil by the difference in specular reflectivity, causing bulk water to appear hotter than bulk oil if their temperatures are the same. (Therefore, there is a certain temperature difference between oil and water for them to appear alike.) On sunny days, however, differential heating causes oil to rise to a higher temperature than the surrounding water because of its higher absorption of solar radiation and lower specific heat, giving rise to the commonly observed contrast of native and crude oil covered sea surfaces in day time remote sensing of oil spills. It has also been observed that a reversal occurs when the oil film is thin, around 50-150 μm. A plausible explanation to this is that since the oil film is thin, it is essentially in thermal equilibrium with the water underneath and thus the oil appears cooler because of its intrinsically lower bulk emissivity. However, this explanation does not account for dark crudes and the possibility that other physical phenomena can play a role. Aside from the thermal equilibrium case, we believe that the contrast variations can arise from thin film interference effect, a well studied subject in many different contexts. In oil spill detection, the only film thickness dependent contrast model we have identified in the literature are in the visible wavelengths [5,6] where thermal emission is negligible, but not in the LWIR. The film thickness dependent contrast is of great importance for correct interpretation of the oil covered area, as well as estimate of the oil film thickness. However, there is relatively little theoretical consideration on this topic and the phenomenon has remained largely unexplained.

In this paper, we investigate the thickness dependent radiance contrast using thin film interference theory. We review two different modeling techniques: indirect method based on Kirchhoff's Law and direct method by summing over volumetric radiators. We show that the optical interference effect plays an important role in the oil-water contrast. In addition, we demonstrate that thickness variation alone can indeed introduce the historically observed contrast reversal, even when the oil is hotter than water.

## 2. Methods

Emissivity (ε) is defined as the fraction a gray body emits relative to a black body at the same temperature. From Kirchhoff's law [7], one can show that the emissivity in a given direction is identical to the absorptivity at the same wavelength if it were incident along the same direction. In addition, based on energy conservation, the reflected (R), transmitted (Tr), and absorbed (emitted, ε) portions of radiance sum to one. Therefore, the emissivity of a surface can be calculated by $\varepsilon = 1 - R - Tr$. Since most crude oils and water are optically thick in the LWIR, *i.e.*, with very high absorption, the penetration depth of infrared light is usually less than 1 cm. When the transmitted light is negligible, the emissivity of bulk oil and water is simply $\varepsilon = 1 - R$. This expression permits determination of emissivity based on reflectance

#96040 - $15.00 USD Received 12 May 2008; revised 17 Jun 2008; accepted 27 Jun 2008; published 30 Jun 2008

and has been termed as the "indirect" method [8]. On the contrary, emissivity can also be calculated directly via radiative transfer theory without using the Kirchhoff's law [9, 10]. The major advantage of the direct approach is that the film and the underlying material can be assigned different temperatures when total radiance is the quantity of interest. We explore the direct method to simulate sustained differential heating effect.

*2.1 Indirect approach*

In the indirect approach, the emissivity of the oil covered water surface can be calculated using the Kirchhoff's Law. Consider an air-oil-water three-stack model shown in Fig. 1, the reflectivity at the air-oil interface is given by:

$$R = \left| \frac{r_{12} + r_{23}\exp(-2i\beta_2)}{1 + r_{12}r_{23}\exp(-2i\beta_2)} \right|^2 \quad , \qquad (1)$$
$$\beta_2 = 2\pi(h/\lambda)\sqrt{\hat{n}_2^2 - \hat{n}_1^2 \sin^2(\theta_1)}$$

where $r$ is the Fresnel interfacial amplitude reflectivity [11] with subscripts $_{ij}$ denoting the direction of wave propagation from medium $i$ to $j$, $\hat{n}_i$ is the complex refractive index of medium $i$, $\theta_1$ is the incident (exiting) angel from the top oil surface, $h$ is the oil film thickness, and $\lambda$ is the wavelength. This approach treats oil and water as a lumped, opaque medium and thus justifies the application of the Kirchhoff's Law. A natural limitation of this approach is that the oil film and water have to be in thermal equilibrium. Thus, differential heating cannot be modeled.

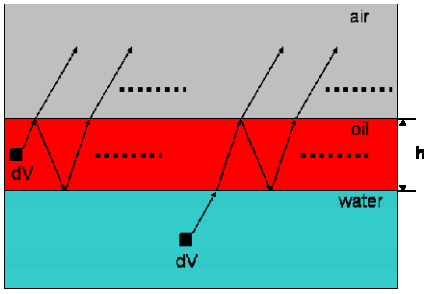


Fig. 1. The air-oil-water stack. The three media are denoted as 1, 2, and 3 in the equations. The thickness of the oil film is h.

*2.2 Direct approach*

In the direct approach, the total emissivity can be considered as the sum of two contributions: the radiance emitted by the water, as seen through the film, and that emitted by the film [8]. In either case, the emitted radiance can be modeled as the collective intensity of waves emitted by volumetric elements. The waves subsequently experience attenuation during propagation, and multiple transmissions and reflections at the interfaces. The attenuation can be accounted for by the Beer's law, and the interfacial amplitude transmissivity and reflectivity can be obtained using Fresnel formulas [11]. For the oil film contribution, the emission can be obtained by integrating the intensity of the waves emitted from individual volumetric elements at position y in the film over the entire film thickness, h:

$$I_{oil} = \frac{\lambda}{4\pi k_2} \left| \frac{t_{12}}{1 - r_{21}r_{23}e^{i(2\pi/\lambda)\hat{n}_2(h/\cos\theta_2)}} \right|^2 (1 - e^{-4\pi k_2 h/\lambda}), \qquad (2)$$

#96040 - $15.00 USD Received 12 May 2008; revised 17 Jun 2008; accepted 27 Jun 2008; published 30 Jun 2008

where $r_{ij}, \hat{n}_i$, and $\lambda$ were defined previously, $t_{ij}$ is the Fresnel interfacial amplitude transmissivity, $k_i$ (the extinction coefficient) is the imaginary part of the complex refractive index $\hat{n}_i$, and $\theta_2$ is the angle of refraction in the film. By definition, the emissivity contributed by the film is obtained by the ratio of the Poynting vectors of the emitted intensity to the original intensity:

$$\varepsilon_{oil} = \mathrm{Re}\left\{\frac{\hat{n}_1}{\hat{n}_2}\right\}\frac{4\pi k_2}{\lambda} I_{oil}\,. \tag{3}$$

Similarly, the emission from the water and the equivalent partial emissivity can be calculated as:

$$\begin{aligned} I_{water} &= \frac{\lambda}{4\pi k_3}\left|\frac{t_{21}t_{32}}{1-r_{21}r_{23}e^{i(2\pi/\lambda)\hat{n}_2(h/\cos\theta_2)}}\right|^2 e^{-4\pi k_2 h/\lambda} \\ \varepsilon_{water} &= \mathrm{Re}\left\{\frac{\hat{n}_1}{\hat{n}_3}\right\}\frac{4\pi k_3}{\lambda} I_{water} \end{aligned}\,. \tag{4}$$

The total emissivity can be calculated by summing the individual contributions from the oil film and the water. On the other hand, since the emissivity is now separated in two parts, total radiance can be calculated as the sum of individual emissivity-Planck products:

$$R_{total} = B(T_{oil})\varepsilon_{oil} + B(T_{water})\varepsilon_{water}\,, \tag{5}$$

with $B$ the Planck's law. This expression allows different temperatures for the water and oil. It can be seen that as the film thickness approaches zero, the total radiance is contributed entirely by the underlying water, while on the other extreme all by the oil film. In the following, we use the model to calculate the contrast of thin oil film covered and native water surfaces for various relative temperatures, oil optical properties, and observation angles. The contrast used here is defined as:

$$C = (R_{oil/water} - R_{water})/R_{water}\,, \tag{6}$$

where $R_{oil/water}$ and $R_{water}$ are the radiance from the oil-covered and the native water surfaces, respectively.

### 3. Optical properties of hydrocarbon constituents and crude oils

Infrared optical properties of key crude oil constituents have been published by the American Petroleum Institute in the 60's [12]. In general, these hydrocarbon constituents have higher real refractive index than water, and show a slowly upward trend from 8 to 14 μm. The extinction coefficient, on the other hand, has multiple peaks corresponding to the molecular vibrational features in a particular constituent. Overall, the extinction coefficients of these constituents are smaller than that of water in the LWIR range. Optical properties of water have been well documented [13] and the real refractive index varies from 1.29-1.11, and the extinction coefficient from 0.034-0.37 as wavelength increases in LWIR. We selected four representative hydrocarbon constituents, including, iso-octane, n-heptane, n-decane, and o-xylene for our calculations. Table I lists the optical properties of these hydrocarbons and water at 8 μm.

#96040 - $15.00 USD Received 12 May 2008; revised 17 Jun 2008; accepted 27 Jun 2008; published 30 Jun 2008

Table I. Optical properties of four hydrocarbon constituents and water at 8 μm.

| | n | k |
|---|---|---|
| Iso-octane | 1.385 | 0.0063 |
| n-heptane | 1.383 | 0.0008 |
| n-decane | 1.405 | 0.0017 |
| o-xylene | 1.491 | 0.001 |
| water | 1.291 | 0.0343 |

Since crude oil is much more complicated than any hydrocarbon constituent, we also acquired absorption spectra of eight different dead oils, including five from the Schlumberger-Doll Research library and three from the Gulf of Mexico. These data were acquired using a Bruker Vertex 70 FTIR spectrometer with a ZnSe attenuated total reflectance (ATR) module. Figure 2 displays the absorption spectra of three representative crude oils.

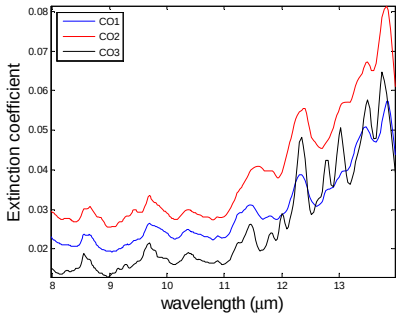


Fig. 2. Absorption spectra of three representative oils.

## 4. Results and discussion

Contrast defined by Eq. (6) was calculated at a single wavelength (8 μm) for different hydrocarbon temperatures and fixed water temperature (293K) with results shown in Fig. 3-6. We observe the upward trend of contrast as thickness increases given sufficient temperature differences. In addition, since contrast reversal is defined as zero-crossing of the blue trace, multiple contrast reversals are clearly identified in all constituents at oil temperature 294K except o-xylene, suggesting that contrast reversal can occur entirely because of thickness variations. Further, the results here demonstrate that the contrast can be negative even when oil is hotter than water as long as the film is thinner than some transition values. When oil film becomes thinner than the transition value, the probability of observing negative contrast increases significantly.

#96040 - $15.00 USD Received 12 May 2008; revised 17 Jun 2008; accepted 27 Jun 2008; published 30 Jun 2008

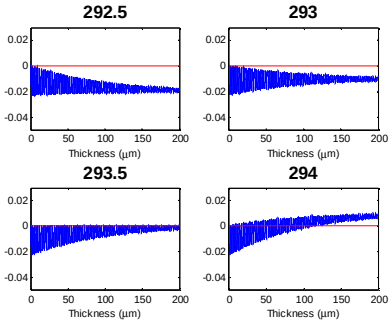


Fig. 3. Contrast (Eq. (6)) for different iso-octane temperatures (292.5-294K). Water temperature was fixed at 293K and 8 μm wavelength was used in all calculations.

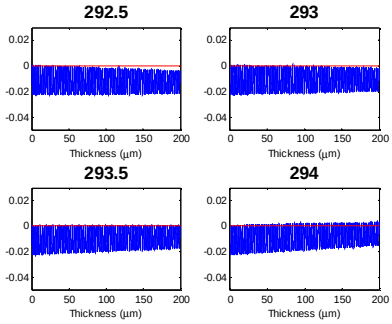


Fig. 4. Contrast (Eq. (6)) for different n-heptane temperatures (292.5-294K). Water temperature was fixed at 293K and 8 μm wavelength was used in all calculations.

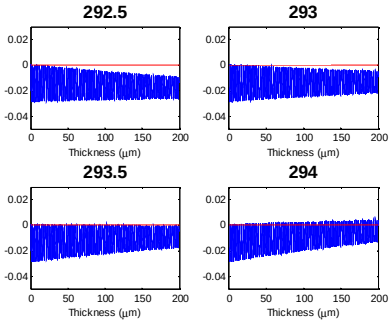


Fig. 5. Contrast (Eq. (6)) for different n-decane temperatures (292.5-294K). Water temperature was fixed at 293K and 8 μm wavelength was used in all calculations.

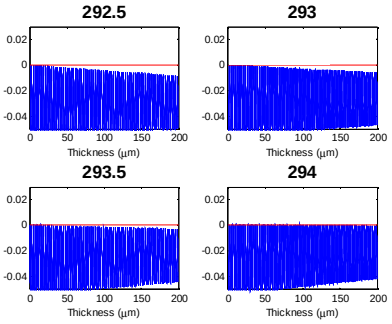


Fig. 6. Contrast (Eq. (6)) for different o-xylene temperatures (292.5-294K). Water temperature was fixed at 293K and 8 μm wavelength was used in all calculations.

Figure 7 shows the observation angle dependence of the contrast. Since the Fresnel coefficients are highly polarization dependent, we use different color to denote various polarization states. We observe that the contrast reversal shifts toward larger film thickness for unpolarized light and further departure of the two polarization states, as the observation angle deviates from nadir. To examine how contrast varies spectrally, we selected 4 different wavelengths for iso-octane. Because the optical properties at these four wavelengths (listed in each plot) are different, quite different results are observed in Fig. 8. Not only the steady state values are different, the transition thickness is dictated by the extinction coefficient of the hydrocarbon.

For the above calculations, monochromatic light source was assumed. For measurements taken using commercial thermal cameras which integrate over the wavelengths between 8-14 μm, the relative phase shift among various wavelengths will reduce the amplitude of the interference fringes. To simulate measurements taken using a range of wavelengths, we calculated the contrast over the full range of 8-14 μm with 0.2 nm step size and display the results in Fig. 9. We observe that the spectral averaging effect not only reduces the amplitude of the interference fringes, but also generates beating. Similar to the single wavelength calculations, multiple contrast reversals are observed. However, compared to results from

#96040 - $15.00 USD Received 12 May 2008; revised 17 Jun 2008; accepted 27 Jun 2008; published 30 Jun 2008

single wavelength calculations, these contrast reversals are localized in a narrower thickness range, corresponding to a tighter range of transition thicknesses.

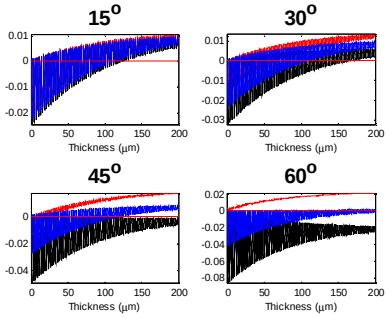


Fig. 7. Contrast for different observation angles and polarizations: red, p-polarized; black, s-polarized; blue, unpolarized. Iso-octane at 8 μm wavelength is used as an example.

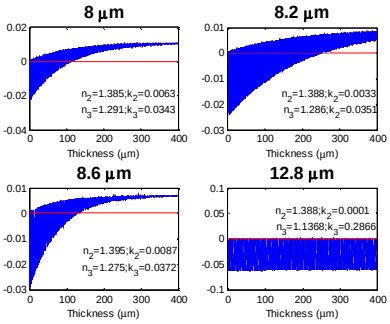


Fig. 8. Contrast at different narrow wavelength bands for iso-octane at 294K: 8, 8.2, 8.6, and 12.8 μm.

Moreover, the results presented here are based on the assumption that the film thickness is uniform. In practical thermal imaging, intensity measured by a particular detector element is usually an averaged value from a much larger area in the image plane, where a distribution of film thickness exists. In addition, natural factors such as ocean waves and wind can create additional non-uniformities in film thicknesses. The collective effect of mechanisms mentioned above can "smear" the interference fringes and cause the fast-fluctuating wiggles to diminish. Therefore, it is most likely that the upward trend can be observed, which results in contrast reversal at a single transition thickness. To simulate that, we applied a Savitzky-Golay smoothing algorithm with a range of 20 μm. The result plotted in Fig. 10 shows a much smoother contrast curve and a transition thickness within a few microns accuracy.

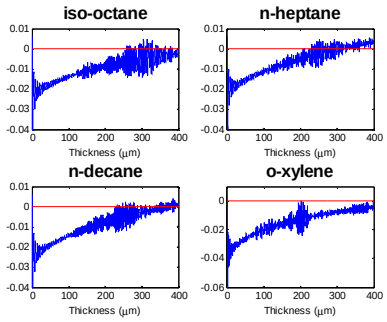


Fig. 9. Contrast using integrated wavelength band from 8-14 μm (0.2 nm step size) for the four representative hydrocarbon constituents at 295K.

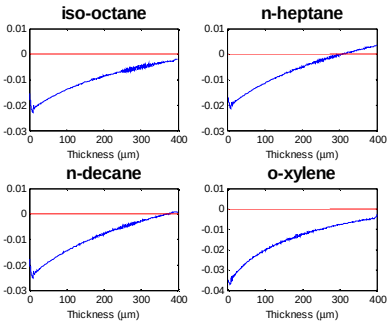


Fig. 10. Results in Fig. 8 smoothed using a Savizky-Golay filter with 20 μm window, simulating non-uniform film thickness.

To apply this model on real crude oils, we calculated the contrast using the acquired crude oil spectra as shown in Fig. 2. Because highly specialized instrument is needed for index measurement in our wavelength range of interest, we used two values close to that reported in ref. 14, the only value we have identified in the literature [14]. In Fig. 11, we observe very smooth contrast curves for all oil samples, and a single transition thickness. The interference effect is more pronounced for oil film thickness less than 50 μm. The transition thickness plot

#96040 - $15.00 USD Received 12 May 2008; revised 17 Jun 2008; accepted 27 Jun 2008; published 30 Jun 2008

shows a transition range of ~30-100 μm. In addition, it indicates that the larger the refractive index difference between oil and water, the larger the transition thickness, and the lower the steady state contrast. Similar to crude oil properties, variations in water salinity and environmental temperature/humidity might change the calculated results, however, not in a significant way.

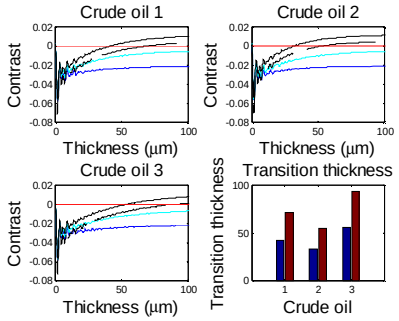


Fig. 11. Contrast (Eq. (6)) for three different crude oils. Refractive index was fixed at 1.45 for all solid curves: blue, oil 293K; cyan, oil 294K; black, oil 295K. Refractive index was 1.5 for the dashed curves with oil at 295K. Water was fixed at 293K for all curves. In the transition thickness plot, the blue bars are for index 1.45, and the red bars are for index 1.5.

In principle, the transition thickness can be calculated by equating the water radiance and the radiance from the oil covered surface. However, owing to the complexity of the equation, an analytical solution is not easily obtainable. In our calculations, a fundamental assumption is that differential heating is sufficient to maintain the assigned temperature differences. This might indeed not hold for extremely thin light oil films. On the other hand, as the film thickness grows, the temperature difference may increase owing to stronger differential heating. However, these competing effects will simply cause the transition thickness for contrast reversals to shift leftward, *i.e.*, towards thinner film thickness.

The results here support the historically observed thickness dependent contrast reversal in oil covered sea surfaces. In addition, they provide evidence that contrast reversal can occur with the presence of differential heating because of the role of thin film interference.

## 4. Conclusion

In conclusion, we have developed an analytical model to describe the well known, phenomenon of infrared radiance contrast reversal that occurs at transition film thickness in crude oil covered water surfaces. This model is based on interference theory and the direct approach in radiative transfer theory, and therefore is capable of modeling daytime differential heating between oil and water. We demonstrate contrast reversal entirely based on oil film thickness variations. Influential parameters such as relative temperature, crude oil optical properties, and observation angle were also studied using the model.

## Acknowledgments

The authors thank Matthew Clayton, Martin Hurlimann, Martin Poitzsch, and Yi-Qiao Song for general discussions on this manuscript and generous support to this project. We thank Fred Morris for assistance of acquiring the FTIR data.

#96040 - $15.00 USD Received 12 May 2008; revised 17 Jun 2008; accepted 27 Jun 2008; published 30 Jun 2008